Optimization of Operational Performance Indicators of a Power Plant with a Gas-Liquid Fuel Supply System. Part I

Lysenko R. D., Ryaboshapka V. B.

Vinnytsia National Agrarian University
Vinnytsia, Ukraine

Abstract. The main objectives of this study were to determine the maximum replacement of conventional diesel fuel with liquefied petroleum gas in a production diesel engine operating in dual-fuel mode, with diesel providing pilot ignition and gas serving as the primary fuel, ensure stable operation across all load and speed conditions, and assess the influence of pilot and gaseous fuel quantities on engine performance. These objectives were achieved by analysing diesel conversion methods, gas supply control and existing mathematical models, developing diesel and dual-fuel cycle models based on the Wiebe function with a variable combustion shape parameter, and computationally investigating how the fuel substitution coefficient affects heat release, cylinder pressure and temperature. The most important results include identification of differences in combustion and heat release between diesel and dual-fuel cycles, including lower calculated pressure and higher temperature in dual-fuel operation under the adopted modelling conditions, and determination of relationships describing changes in the combustion shape parameter, heat release fraction and rate, cylinder pressure and temperature as diesel fuel is replaced by liquefied petroleum gas in a naturally aspirated engine.
The significance of the results lies in establishing analytical relationships between combustion characteristics, liquid and gaseous fuel quantities supplied per cycle and engine cycle parameters, providing a basis for model refinement, development of gas supply and pilot fuel quantity control systems and algorithms, and assessment of fuel and energy efficiency over the investigated operating range.
Keywords: dual-fuel engine, liquefied petroleum gas, external mixture formation, pilot injection, heat release, fuel efficiency, energy efficiency.

DOI: https://doi.org/10.52254/1857-0070.2026.4-72.17
UDC: 621.431.7:662.767:620.92

Optimizarea indicatorilor de performanță operațională ai unei unități energetice cu sistem de alimentare cu combustibil gazos și lichid. Partea I

Lîsenko R. D., Reaboșapka V. B.
Univesitatea Agrară din Vinnița

Rezumat. Obiectivele principale ale acestui studiu au fost: determinarea gradului maxim de înlocuire a motorinei convenționale cu gaz petrolier lichefiat (GPL) într-un motor diesel care funcționează în regim mixt (dual-fuel) — unde motorina asigură aprinderea pilot, iar gazul servește drept combustibil principal; asigurarea unei funcționări stabile în toate regimurile de sarcină și turație; și evaluarea influenței cantităților de combustibil pilot și gazos asupra performanțelor motorului. Aceste obiective au fost atinse prin: analizarea metodelor de conversie a motoarelor diesel, a controlului alimentării cu gaz și a modelelor matematice existente; dezvoltarea unor modele pentru ciclurile diesel și mixte, bazate pe funcția Wiebe cu un parametru variabil de formă a arderii; și investigarea computațională a modului în care coeficientul de substituție a combustibilului influențează degajarea de căldură, precum și presiunea și temperatura din cilindru. Cele mai importante rezultate includ: identificarea diferențelor în procesele de ardere și degajare a căldurii între ciclurile diesel și cele mixte (în condițiile de modelare adoptate, regimul mixt prezintă o presiune calculată mai scăzută și o temperatură mai ridicată); precum și stabilirea unor relații care descriu variațiile parametrului de formă a arderii, fracțiunii și vitezei de degajare a căldurii, presiunii și temperaturii din cilindru pe măsură ce motorina este înlocuită cu gaz petrolier lichefiat într-un motor cu aspirație naturală. Semnificația rezultatelor constă în stabilirea unor relații analitice între caracteristicile arderii, cantitățile de combustibil lichid și gazos furnizate pe ciclu și parametrii ciclului motor. Acestea oferă o bază pentru rafinarea modelelor, dezvoltarea sistemelor și algoritmilor de control al alimentării cu gaz și al cantității de combustibil pilot, precum și pentru evaluarea eficienței energetice și a consumului de combustibil în gama de funcționare analizată.

© Lîsenko R. D., Reaboșapka V. B.
2026

Cuvinte-cheie: motor cu alimentare mixtă (dual-fuel), gaz petrolier lichefiat, formarea amestecului în exteriorul cilindrului, injecție pilot, degajare de căldură, eficiența consumului de combustibil, eficiență energetică.

Оптимизация эксплуатационных показателей энергетической установки с газожидкостной системой питания. Часть I

Лысенко Р.Д., Рябошапка В. Б.

Винницкий Национальный аграрный университет, Винница, Украина

Аннотация. Основные цели исследования это выявление максимального замещения традиционного дизельного топлива сжиженным нефтяным газом в качестве альтернативного топлива, используя газодизельный цикл для работы серийного дизельного двигателя, при использовании стандартного дизельного топлива в качестве запальной дозы, а сжиженного нефтяного газа – в качестве основного; обеспечение стабильной работы двигателя с использованием альтернативного топлива на всех нагрузочно-скоростных режимах; выявление влияния запальной дозы и альтернативного топлива на технико-эксплуатационные параметры энергетической установки. Эти цели были достигнуты путём анализа способов переоборудования дизелей, регулирования газоподачи и существующих математических моделей, разработки математической модели дизельного и газодизельного циклов на основе модели Вибе И. И. с переменным показателем характера сгорания, а также расчётного исследования влияния коэффициента замещения дизельного топлива сжиженным нефтяным газом на тепловыделение, давление и температуру в цилиндре. Наиболее важные результаты включают выявление различий в характере сгорания и тепловыделения в дизельном и газодизельном циклах, в частности получение при принятых условиях моделирования расчётных значений более низкого давления и более высокой температуры в газодизельном цикле; определение закономерностей изменения показателя характера сгорания для газодизельного цикла, доли и скорости тепловыделения, давления и температуры; расчётное установление влияния замещения части дизельного топлива сжиженным нефтяным газом на рабочий процесс дизельного двигателя без наддува. Значимость полученных результатов заключается в установлении аналитических связей между характеристиками сгорания, цикловой подачей жидкого и газообразного топлива и показателями рабочего цикла двигателя, что создаёт основу для дальнейшего уточнения модели газодизельного рабочего процесса, разработки устройств и алгоритмов регулирования газоподачи и запальной дозы, а также оценки топливной и энергетической эффективности установки в исследованном диапазоне режимов.

Ключевые слова: газодизельный двигатель, сжиженный нефтяной газ, внешнее смесеобразование, запальная доза, тепловыделение, топливная эффективность, энергетическая эффективность.

1. INTRODUCTION

Converting diesel internal combustion engines to alternative fuels, particularly liquefied petroleum gas (LPG) and compressed natural gas (CNG), is considered a means of reducing diesel fuel consumption and environmental impact.

Conversion approaches differ in mixture formation, operating cycle and gas-supply control [1, 2, 3].

For agricultural diesel engines, maintaining the original performance after conversion to a dual-fuel supply system is important.

In dual-fuel operation, the gas–air mixture is ignited by a pilot quantity of liquid fuel.

Conversion therefore requires coordination of both fuel supply and the governor of the high-pressure fuel injection pump.

These relationships must be investigated to select the diesel substitution level and ensure stable operation under variable loads [2, 3].

2. LITERATURE REVIEW, RESEARCH AND APPROACHES TO DUAL-FUEL ENGINE OPERATION

Hall and Kassa [23] reviewed combustion control approaches for dual-fuel engines operating on natural gas and diesel fuel. The conversion, mixture-formation and fuel-supply control approaches considered in this article are summarised in Table 1 using the relevant publications.

2.2.2. Liquefied petroleum gas (LPG)

Aydin M. et al. [2] investigated dual-fuel operation of a single-cylinder diesel generator with gaseous LPG supplied to the intake manifold, i.e. external mixture formation. Mohsen J. M. and Al-Dawody M. F. [3] modelled partial diesel substitution by LPG in Diesel-RK. The experimental studies by Toledo E. et al. [7] and Tchato Yotchou G. V. et al. [8] concerned performance, emissions and combustion characteristics at different loads and fuel ratios.

Table 1

Summary of dual-fuel engine operation

№	Conversion approaches		Publications
1	Conversion of a diesel engine to a gas engine		[1], [4]
2	Dual-fuel operation with external gas–air mixture formation	Compressed natural gas (CNG) operation	[5], [6]
		Liquefied petroleum gas (LPG) operation	[2, 3, 7, 8]
3	Internal mixture formation and direct fuel injection	LPG; other direct fuel-supply approaches	[9, 10, 11]
		Natural gas; assisted ignition	[18]
4	Gas-supply control methods	Automatic	[12, 15, 17]
		Mechanical	[14, 16]

2.3. Internal mixture formation

2.3.1. LPG and other fuel-supply approaches

Maza Rubina A., and Lastra Espinoza L. [9] considered internal mixture formation with LPG supplied through the high-pressure fuel line and compared calculated and experimental engine characteristics.

Dual direct injection of fuels with different reactivities represents a separate approach [10]. Gas supply during the compression stroke in low-speed marine dual-fuel engines was investigated in [11]. These approaches differ in fuel type, injection-system design and conditions of fuel delivery to the cylinder.

2.3.2. Direct natural gas injection

Willi's patent [18] proposed controlling the direct-injection pressure of natural gas according to load. At low loads, reduced pressure increases injection duration for a given gas quantity and improves combustion conditions.

Assisted ignition is provided, particularly by a glow plug; diesel pilot ignition is an additional implementation option. Table 1 presents this patent as a solution for an engine with direct gas injection.

2.4. Gas-supply control methods and systems

2.4.1. Automatic electronic systems

Electronic systems provide operating-point-dependent gas metering and mode switching [12, 13]. The pilot-quantity corrector [15] allows diesel and gas supplies to be coordinated. In [17], a programmable logic controller (PLC) was used to control the two fuels separately. Such systems require appropriate sensors and actuators.

2.4.2. Mechanical systems

Mechanical solutions include a pneumatic corrector [14] and coordination of the fuel-pump and throttle levers [16]. Their application requires consideration of the standard governor's effect on the pilot-fuel quantity. The interaction between the governor and gas supply must therefore be verified when converting a production diesel engine.

The Wiebe I. I. model [19, 20] is easy to apply but requires experimental selection of the exponent m. The Razleytsev–Kulikov model [3, 21] describes injection and combustion in greater detail and requires additional fuel-supply data (Table 2).

2.6. Unresolved issues and differences from previous results

The studies reviewed show that the use of LPG in dual-fuel cycles, pilot-ignition quantity control and combustion modelling already has a theoretical and experimental basis [3, 7, 8, 15, 19 – 23]. However, results obtained with different mixture-formation methods, control systems and operating conditions cannot determine the gas and pilot-ignition settings of a particular naturally aspirated production engine without further justification.

2.5. Mathematical modelling of combustion

The relationship between fuel supply and load and speed characteristics still needs to be established for the investigated installation.

Existing electronic correctors regulate the pilot-fuel quantity according to speed [15], whereas mechanical systems coordinate liquid- and gaseous-fuel control [14, 16]. However, the effect of the constant-speed governor in the high-pressure pump requires separate verification for the selected conversion approach: the resulting changes in diesel supply complicate evaluation of an increase in gas supply.

The modelling methods are summarized in Table 2.

Table 2

Approaches and methods for modelling combustion in diesel and dual-fuel cycles

No.	Mathematical model	Main equations and formulas describing the model	References
1	I. I. Wiebe exponential model describing heat-release curves	$x = 1 - e^{C_z \cdot \left(\frac{\varphi}{\varphi_z}\right)^{m+1}}$ $C_z = \ln(1 - x_z)$ $\frac{dx}{d\varphi} = -C(m+1)\left(\frac{\varphi}{\varphi_z}\right)^m \cdot e^{C\left(\frac{\varphi}{\varphi_z}\right)^{m+1}}$	[19, 20]
2	Razleytsev–Kulikov model describing combustion	$\tau = e^{\left(\frac{Ea}{8.312T} - \frac{70}{CN+25}\right)} \cdot \sqrt{\frac{T}{P}} \cdot 3.8 \cdot 10^{-6} \cdot \left(n \cdot 1 \cdot -1.6 \cdot 10^{-4}\right)$ $\frac{dx}{d\tau} = \varphi_1 \left\{\frac{d\sigma_u}{d\tau}\right\} + \left\{A_0 \cdot (0{,}1\sigma_{ud} + x_0)(\sigma_{ud} - x_0)\left(\frac{m_f}{V_i}\right)\right\} \cdot \varphi_0$ $\frac{dx}{d\tau} = \varphi_2 \cdot \left\{(\varnothing - x)(\sigma_u - x) \cdot \left\{\frac{mf}{V_c}\right\} \cdot A_2\right\} + \varphi_1 \cdot \left\{\frac{d\sigma_u}{d\tau}\right\}$ $\frac{dx}{d\tau} = K_T \cdot A_3 \cdot (\varepsilon_b \varnothing - x)(\sigma_u - x) \cdot \varphi_3$	[3, 21]
3	Filipkovsky model with a variable combustion-shape exponent	$\frac{dx}{d\tau} = -C \exp\left(C\varphi^{m+1}\right) \frac{1}{\varphi_z}\left[(m+1)\varphi^m + \varphi^{m+1} \ln\varphi \frac{dm}{d\varphi}\right]$	[22]
4	A. P. Kuzmenko model for determining the variable combustion exponent in a gas engine	$m_i = 10{,}639 \cdot \bar{\varphi}_i \cdot (\lambda_g + 0{,}00025) \cdot \frac{\theta + 18}{40} \cdot$ $\cdot \frac{\eta_v - 0{,}25}{0{,}8} \cdot \frac{\varepsilon + 1}{11} \cdot \frac{n + 500}{5000} -$ $-28{,}025 \cdot \bar{\varphi}_i^2 + 98{,}045 \cdot \bar{\varphi}_i^3 - 156{,}86 \cdot \bar{\varphi}_i^4 + 86{,}88 \cdot \bar{\varphi}_i^5$	[25]

The research question is therefore to determine diesel substitution in dual-fuel operation at the rated operating point and the conditions for maintaining brake power.

The theoretical part of this task concerns selecting a combustion description suitable for the available input data. The I. I. Wiebe model requires justification of the combustion exponent, whereas detailed models require additional information on injection and fuel supply [3, 19–21]. For the investigated engine, the assumed substitution level must be taken into account and its effect on calculated heat release and indicated parameters assessed. Applying the established mathematical framework to these conditions requires justification of the input parameters and a distinction between calculated and experimentally established relationships.

This work differs from the reviewed approaches by investigating the dual-fuel process in a naturally aspirated production engine with external LPG mixture formation at a substitution coefficient $k_r = 0.5$. Unlike studies of a specified speed characteristic of the pilot quantity using an electronic corrector [15], in which non-engine tests of the device did not reveal the governor's effect on the substitution coefficient in a dual-fuel engine, this study considered theoretical combustion relationships for this engine type and their effect on k_r and established its maximum possible value through engine tests. The contribution includes the load and speed relationships obtained under these conditions and the experimental fuel-consumption ratio while maintaining power output. Comparison of combustion characteristics calculated using the I. I. Wiebe model with a variable exponent against the experimental curve confirms the adequacy of the developed model for this engine type and its

use to investigate the dual-fuel cycle in the same engine, as performed here. The results showed that, when switching to dual-fuel operation, the heat released per cycle during replacement of diesel fuel by gaseous fuel does not correspond to the substitution coefficient, requiring an adjustment that was made during the experiments. These results provide a basis for further coordination of gas supply and pilot-fuel quantity within the investigated operating range.

3. AIM, OBJECTIVES AND RESEARCH METHODS

The aim is to optimise the operating characteristics of a power unit with a gas–liquid fuel system. The objectives are to provide a theoretical basis for the need to adjust the pilot quantity and its effect on diesel substitution by gaseous fuel through combustion and heat-release modelling; conduct engine tests; and determine the LPG substitution level. The methods include the I. I. Wiebe model with variable *m* and bench tests of the 4Ch11.0/12.5 engine.

4. OBJECT OF THE STUDY

The object of the study is a 4Ch11.0/12.5 diesel engine with a gas–liquid fuel supply system (Table 3).

Table 3

Technical specifications of the test engine

Parameter	Value
Engine model	D-240 (4Ch11.0/12.5)
Engine type	Four-cylinder naturally aspirated diesel
Number of cylinders	4
Cylinder bore (mm)	110
Piston stroke (mm)	125
Rated speed (rpm)	2200
Compression ratio	16
Investigated operating modes	Diesel and dual-fuel
Mixture formation in dual-fuel operation	External mixture formation
Gas–air mixture ignition method	Diesel pilot quantity

5. MATHEMATICAL MODEL OF COMBUSTION AND THE WORKING PROCESS IN DIESEL AND DUAL-FUEL OPERATION

The Wiebe I.I. model with a variable combustion exponent was used for the 4Ch11.0/12.5 engine.

The heat-release fraction *x* is calculated using [19]:

$$x = 1 - e^{C_z \left(\frac{\varphi}{\varphi_z}\right)^{m+1}} \quad (1)$$

where C_z the combustion constant depends on the fraction of fuel burned by the end of combustion; m is the combustion exponent in the I. I. Wiebe model; φ_z is the combustion duration in crank-angle degrees.

The combustion constant C_z is determined as:

$$C_z = \ln(1 - x_z) \quad (2)$$

where x_z is the fraction of fuel burned at the actual completion of the combustion process.

The combustion duration φ_z is determined using the formula of B. A. Sharoglazov and M. F. Farafontov:

$$\varphi_z = 135 \cdot \lambda^{-1,36} + 25 \quad (3)$$

New relationships for combustion and the working cycle of the 4Ch11.0/12.5 engine were obtained on the basis of known relationships from internal combustion engine theory.

The excess-air ratio for the diesel engine is:

$$\lambda_d = \frac{2{,}1 \cdot 10^5 \cdot \pi \cdot D^2 \cdot S \left\{ p_0 \cdot \varphi_{c.ad} \cdot \varepsilon \left[1 - \frac{3{,}024557 \cdot 10^{-8} \cdot (\beta_{in}^2 + \xi_{in}) \cdot n^2 \cdot \pi^2 \cdot S^2 \cdot D^4 \cdot (1 + \alpha^2)}{h_v^2 \cdot (d_n \cdot \cos\alpha_v + h_v \cdot \alpha_v \cdot \cos^2\alpha_v)^2 \cdot T_0} \right] - \varphi_c \cdot p_r \right\}}{(\varepsilon - 1) \cdot (T_0 + \Delta T) \cdot V_{fc} \cdot \rho_f \left[\frac{C}{3} + H + \frac{1}{8} \cdot (S - O) \right] \cdot R} \quad (4)$$

where the following are represented:

- engine design parameters: D is the cylinder bore, m; S is the piston stroke, m; ε is the

compression ratio; α is the crank–connecting rod mechanism constant; h_v is the intake-valve lift, m; d_n is the intake-port throat diameter, m; α_v is the valve-seat angle, rad;

- engine design and operating parameters: $\phi_{c.ad}$ is the cylinder aftercharging coefficient due to delayed intake-valve closing; φ_c is the cylinder scavenging coefficient due to valve overlap; β_{in} is the charge-velocity attenuation coefficient in the cylinder section considered; ξ_{in} is the intake-system resistance coefficient referred to its narrowest cross-section; ΔT is the charge temperature increase during intake, °C.

The excess-air ratio for the dual-fuel engine is:

- engine operating parameters: p_r is the residual-gas pressure; n is the crankshaft speed, min^{-1}; v_{fc} is the volumetric fuel delivery per cycle, mm³/cycle;
- fuel physicochemical characteristics: is the liquid-fuel density, kg/m³; C, H, S and O are the mass fractions of carbon, hydrogen, sulphur and oxygen, respectively;
- fresh cylinder-charge parameters: $p_0 T_0$ are the ambient-air pressure (MPa) and temperature (K), respectively; R is the universal gas constant, $R = 8.314$ kJ/(kmol·K).

$$\lambda_{gd} = \frac{2{,}1\cdot 10^5 \cdot \pi \cdot D^2 \cdot S \cdot T_0 \cdot \left\{ p_0 \cdot \varphi_{c.ad} \cdot \varepsilon \cdot \left[1 - \frac{3{,}024557\cdot 10^{-8} \cdot \left(\beta_{in}^2 + \xi_{in}\right) \cdot n^2 \cdot \pi^2 \cdot S^2 \cdot D^4 \cdot \left(1+\alpha^2\right)}{h_v^2 \cdot \left(d_n \cdot \cos\alpha_v + h_v \cdot \alpha_v \cdot \cos^2\alpha_v\right)^2 \cdot T_0} \right] - \varphi_c \cdot p_r \right\}}{(\varepsilon - 1)\cdot (T_0 + \Delta T)\cdot V_{fc} \cdot \rho_f \cdot \left\{ 1{,}078 \cdot \left[\frac{C}{3} + H + \frac{1}{8}\cdot (S - O) \right] \cdot R \cdot T_0 \cdot (1 - k_r) + k_r \cdot 194{,}88 \cdot \left[339 \cdot C + 1030 \cdot H - 109 \cdot (O - S) \right] \right\}} \quad (5)$$

where k_r is the coefficient of diesel-fuel substitution by gaseous fuel.

The diesel-cycle exponent m is approximated by a sixth-order polynomial:

$$m = b_1 \cdot \varphi^6 - b_2 \cdot \varphi^5 + b_3 \cdot \varphi^4 - b_4 \cdot \varphi^3 + b_5 \cdot \varphi^2 - b_6 \cdot \varphi + b_7 \quad (6)$$

where φ is the engine crank angle measured from the start of visible combustion, °CA.

$b_1 - b_7$ are polynomial coefficients that depend on the engine operating mode and fu

The excess-air ratio for the hypothetical gas engine is:

$$\lambda_g = \frac{9{,}7965\cdot 10^4 \cdot \pi \cdot D^2 \cdot S \cdot T_0 \cdot \left\{ p_0 \cdot \varphi_{c.ad} \cdot \varepsilon \cdot \left[1 - \frac{3{,}024557\cdot 10^{-8} \cdot \left(\beta_{in}^2 + \xi_{in}\right) \cdot n^2 \cdot \pi^2 \cdot S^2 \cdot D^4 \cdot \left(1+\alpha^2\right)}{h_v^2 \cdot \left(d_n \cdot \cos\alpha_v + h_v \cdot \alpha_v \cdot \cos^2\alpha_v\right)^2 \cdot T_0} \right] - \varphi_c \cdot p_r \right\}}{p_0 \cdot (\varepsilon - 1)\cdot (T_0 + \Delta T)\cdot V_{fc} \cdot \rho_f \cdot \left[339 \cdot C + 1030 \cdot H - 109 \cdot (O - S) \right]} \quad (7)$$

Equations (4–7) apply to high-speed naturally aspirated diesel engines of the 4Ch11.0/12.5 type, with a pear-shaped mixture-formation chamber in the piston, a five-hole nozzle and volumetric-film mixture formation. The equations can also be used for other sizes of high-speed naturally aspirated diesel engine, but this requires the approximating polynomial in Equation (6), obtained by analysing experimental indicator diagrams of the particular engines, or a known value or variation of the combustion-shape exponent m.

Substituting the design, operating, combined design and operating, fuel physicochemical and fresh-charge parameters for the rated operating mode of the 4Ch11.0/12.5 engine, at $n = 2200$ rpm and a compression ratio $\varepsilon = 16$, into Equations (4), (5) and (7) gives the following excess-air ratios: for the diesel cycle, $\lambda_d = 1{,}51$, within the permissible range for high-speed automotive and tractor diesels with either volumetric mixture formation ($\lambda = 1.5\ldots1.8$) or film mixture formation ($\lambda = 1.45\ldots1.55$) [13]; for the dual-fuel cycle, $\lambda_{gd} = 1.54$ and for the hypothetical gas cycle with gas delivery per cycle corresponding to the dual-fuel cycle, $\lambda_g = 1.58$.

Substituting the obtained excess-air ratios into Equation (3) gives the combustion durations: for the diesel cycle, $\varphi_{zd} = 102$ °CA; for the dual-fuel cycle, $\varphi_{zgd} = 99.8$ °CA; and for the hypothetical gas cycle, $\varphi_g = 97.3$ °CA.

Thus, Equations (4), (5) and (7) were used to investigate the range of excess-air ratios for the 4Ch11.0/12.5 engine, with the specified compression ratio $\varepsilon = 16$, at the rated speed $n = 2200$ rpm for the diesel, dual-fuel and hypothetical gas cycles. Substitution of the corresponding λ values into Equation (3) yielded a combustion-duration range of 97.3–102 °CA for these cycles of the investigated engine. Shorter combustion durations correspond to higher coefficients and vice versa, indicating that an increased excess-air ratio reduces combustion duration.

To account for other important factors affecting combustion, including injection timing, the sixth-order polynomial of the I. I. Wiebe combustion-shape exponent m (6) is used. Its variation was investigated in previous work through analysis of experimental indicator diagrams and heat-release curves for the rated mode of the 4Ch11.0/12.5 engine, with $\varepsilon = 16$ at $n = 2200$ rpm and the manufacturer-recommended fuel-delivery advance angle $\varphi_{fs} = 26$ °CA before top dead centre, which also determines the injection advance angle. The coefficients of polynomial (6) were: $b_1 = 4.6356672865 \cdot 10^{-30}$;

$b_2 = 9.868196676314 \cdot 10^{-32}$;

$b_3 = 8.26629672852353 \cdot 10^{-34}$;

$b_4 = 3.46001472767643 \cdot 10^{-35}$;

$b_5 = 7.74144657194142 \cdot 10^{-35}$;

$b_6 = 9.75561964770009 \cdot 10^{-2}$;

$b_7 = 4.93690990913365 \cdot 10^{-2}$.

The variable exponent m for the gas engine is determined using the equation proposed by A.P.Kuzmenko [25], taking Equation (7) into account:

The variable exponent m for the gas engine is:

$$m_i = 10,639 \cdot \frac{\varphi_i}{\varphi_z} \cdot \left(\frac{9,7965 \cdot 10^4 \cdot \pi \cdot D^2 \cdot S \cdot T_0 \cdot \left\{ p_0 \cdot \varphi_{c.ad} \cdot \varepsilon \cdot \left[1 - \frac{3,024557 \cdot 10^{-8} \cdot \left(\beta_{in}^2 + \xi_{in} \right) \cdot n^2 \cdot \pi^2 \cdot S^2 \cdot D^4 \cdot \left(1 + \alpha^2 \right)}{h_v^2 \cdot \left(d_n \cdot \cos\alpha_v + h_v \cdot \alpha_v \cdot \cos^2 \alpha_v \right)^2 \cdot T_0} \right] - \varphi_c \cdot p_r \right\}}{p_0 \cdot (\varepsilon - 1) \cdot (T_0 + \Delta T) \cdot V_{fc} \cdot \rho_f \cdot \left[339 \cdot C + 1030 \cdot H - 109 \cdot (O - S) \right]} + 0,00025 \right) \cdot$$

$$\cdot \frac{\theta + 18}{40} \cdot \left\{ \frac{T_0 \cdot \left\{ p_0 \cdot \varphi_{c.ad} \cdot \varepsilon \cdot \left[1 - \frac{3,024557 \cdot 10^{-8} \cdot \left(\beta_{in}^2 + \xi_{in} \right) \cdot n^2 \cdot \pi^2 \cdot S^2 \cdot D^4 \cdot \left(1 + \alpha^2 \right)}{h_v^2 \cdot \left(d_n \cdot \cos\alpha_v + h_v \cdot \alpha_v \cdot \cos^2 \alpha_v \right)^2 \cdot T_0} \right] - \varphi_c \cdot p_r \right\}}{0,8 \cdot p_0 \cdot (\varepsilon - 1) \cdot (T_0 + \Delta T)} - 0,3125 \right\} \cdot \frac{\varepsilon + 1}{11} \cdot \quad (8)$$

$$\cdot \frac{n + 500}{5000} - 28,025 \cdot \left(\frac{\varphi_i}{\varphi_z} \right)^2 + 98,045 \cdot \left(\frac{\varphi_i}{\varphi_z} \right)^3 - 156,86 \cdot \left(\frac{\varphi_i}{\varphi_z} \right)^4 + 86,88 \cdot \left(\frac{\varphi_i}{\varphi_z} \right)^5$$

where θ is the ignition advance angle; φ_i is the current crank angle measured from the start of visible combustion.

Equation (7) accounts for the actual excess-air ratio, which depends on the design, operating, combined design and operating, fuel physicochemical and fresh-charge parameters for the hypothetical gas cycle at the rated operating mode of the 4Ch11.0/12.5 engine, with $n = 2200$ rpm and $\varepsilon = 16$. In this case, the excess-air ratio was $\lambda_g = 1.58$.

Using Equations (6) and (8), and assuming that the combustion-shape exponent in the dual-fuel cycle takes values characteristic of both the diesel and gas engines, we obtain the following relationships:

$$m_{gd} = (1-k_r)\cdot\left(b_1\cdot\varphi^6 - b_2\cdot\varphi^5 + b_3\cdot\varphi^4 - b_4\cdot\varphi^3 + b_5\cdot\varphi^2 - b_6\cdot\varphi + b_7\right) + k_r \cdot$$

$$\cdot\left[10,639\cdot\frac{\varphi_i}{\varphi_z}\cdot\left(\frac{9,7965\cdot10^4\cdot\pi\cdot D^2\cdot S\cdot T_0\cdot\left\{p_0\cdot\varphi_{c.ad}\cdot\varepsilon\cdot\left[1-\frac{3,024557\cdot10^{-8}\cdot\left(\beta_{in}^2+\xi_{in}\right)\cdot n^2\cdot\pi^2\cdot S^2\cdot D^4\cdot\left(1+\alpha^2\right)}{h_v^2\cdot\left(d_n\cdot\cos\alpha_v + h_v\cdot\alpha_v\cdot\cos^2\alpha_v\right)^2\cdot T_0}\right]-\varphi_c\cdot p_r\right\}}{p_0\cdot(\varepsilon-1)\cdot(T_0+\Delta T)\cdot V_{fc}\cdot\rho_f\cdot\left[339\cdot C+1030\cdot H-109\cdot(O-S)\right]} + 0,0002\right.\right.$$

$$\left.\left.\cdot\left\{\frac{T_0\cdot\left\{p_0\cdot\varphi_{c.ad}\cdot\varepsilon\cdot\left[1-\frac{3,024557\cdot10^{-8}\cdot\left(\beta_{in}^2+\xi_{in}\right)\cdot n^2\cdot\pi^2\cdot S^2\cdot D^4\cdot\left(1+\alpha^2\right)}{h_v^2\cdot\left(d_n\cdot\cos\alpha_v + h_v\cdot\alpha_v\cdot\cos^2\alpha_v\right)^2\cdot T_0}\right]-\varphi_c\cdot p_r\right\}}{0,8\cdot p_0\cdot(\varepsilon-1)\cdot(T_0+\Delta T)} - 0,3125\right\}\cdot\right.\right.$$

$$\left.\cdot\frac{\varepsilon+1}{11}\cdot\frac{n+500}{5000} - 28,025\cdot\left(\frac{\varphi_i}{\varphi_z}\right)^2 + 98,045\cdot\left(\frac{\varphi_i}{\varphi_z}\right)^3 - 156,86\cdot\left(\frac{\varphi_i}{\varphi_z}\right)^4 + 86,88\cdot\left(\frac{\varphi_i}{\varphi_z}\right)^5 - \left(b_1\cdot\varphi^6 - b_2\cdot\varphi^5 + b_3\cdot\varphi^4 - b_4\cdot\varphi^3 + b_5\cdot\varphi^2 - b_6\cdot\varphi + \right.\right. \quad (9)$$

Pressure during compression:

$$p = p_0\cdot\left[1-\frac{(\beta_{in}^2+\xi_{in})\cdot n^2\cdot\pi^2\cdot S^2\cdot D^4\cdot(1+\alpha^2)}{3,024557\cdot10^{-2}\cdot h_v^2\cdot(d_n\cdot\cos\alpha_v + h_v\cdot\alpha_v\cdot\cos^2\alpha_v)^2\cdot T_0}\right]\cdot$$

$$\cdot\left\{\frac{\varepsilon}{\frac{1}{2}\cdot\left[(1-\cos\varphi)+\frac{\alpha}{4}\cdot(1-\cos2\varphi)\right]\cdot(\varepsilon-1)+1}\right\}^{\left(1,41-\frac{100}{n}\right)} \quad (10)$$

Temperature during compression:

$$T = \frac{T_0+\Delta T+\dfrac{\varphi_c\cdot p_r\cdot(T_0+\Delta T)}{\varphi_{c.ad}\cdot\varepsilon\cdot\left[p_0\cdot\left(1-\dfrac{(\beta_{in}^2+\xi_{in})\cdot n^2\cdot\pi^2\cdot S^2\cdot D^4\cdot(1+\alpha^2)}{3,024557\cdot10^{-2}\cdot h_v^2\cdot(d_n\cdot\cos\alpha_v + h_v\cdot\alpha_v\cdot\cos^2\alpha_v)^2\cdot T_0}\right)\right]-\varphi_c\cdot p_r}}{1+\dfrac{\varphi_c\cdot p_r\cdot(T_0+\Delta T)}{\left\{\varphi_{c.ad}\cdot\varepsilon\cdot\left[p_0\cdot\left(1-\dfrac{(\beta_{in}^2+\xi_{in})\cdot n^2\cdot\pi^2\cdot S^2\cdot D^4\cdot(1+\alpha^2)}{3,024557\cdot10^{-2}\cdot h_v^2\cdot(d_n\cdot\cos\alpha_v + h_v\cdot\alpha_v\cdot\cos^2\alpha_v)^2\cdot T_0}\right)\right]-\varphi_c\cdot p_r\right\}\cdot T_r}}\cdot$$

$$\cdot\left\{\frac{\varepsilon}{\frac{1}{2}\cdot\left[(1-\cos\varphi)+\frac{\alpha}{4}\cdot(1-\cos2\varphi)\right]\cdot(\varepsilon-1)+1}\right\}^{\left(0,41-\frac{100}{n}\right)} \quad (11)$$

The total specific utilised heat of combustion is determined from the I. I. Wiebe formula [19], taking the elemental composition of the fuel into account:

$$q_z = \frac{\xi\cdot[339\cdot C+1030\cdot H-109\cdot(O-S)]}{4,184\cdot[(1+\gamma_r)\cdot\lambda\cdot l_{0d}+1]} \quad (12)$$

where ξ is the heat-utilisation coefficient during visible combustion; $\xi = 0.9$ is adopted

.

The total specific utilised heat of combustion for the dual-fuel cycle is determined as:

$$q_{zg} = \frac{\xi \cdot \left[Q_{ld} \cdot G_{fcd} \cdot (1-k_r) + k_r \cdot Q_{lg} \cdot V_{gc} \right]}{4{,}184 \cdot \left(1+\lambda_{gd} \cdot l_{0g}\right) \cdot (1+\gamma_r) \cdot \left[G_{fcd} \cdot 1{,}078 \cdot (1-k_r) + \frac{k_r \cdot 0{,}928 \cdot V_{gc} \cdot p_0 \cdot 10^3}{R \cdot T_0} \right]} \quad (13)$$

Pressure during combustion [19]:

$$p_2 = \frac{0{,}8705 \cdot q_z \cdot \Delta x_{1-2} + 103{,}947 \cdot p_1 \cdot (K_{1-2} \cdot v_1 - v_2)}{K_{1-2} \cdot v_2 - v_1} \quad (14)$$

Temperature during combustion:

$$T_1 = \frac{p_1 \cdot V_x \cdot 10^3}{V_\beta \cdot R} \quad (15)$$

When determining the increase in internal energy, the temperature dependence of heat capacity and the effect of changes in working-fluid composition were included within the adopted empirical approximation. An average heat-capacity ratio was used for each elementary interval of the combustion process [19]:

$$k_{1-2} = 1{,}259 + \frac{76{,}7}{T_{1-2}} - \left(0{,}005 + \frac{0{,}0375}{\lambda}\right) \cdot x_{1-2} \quad (16)$$

The heat-capacity factor is determined from the heat-capacity ratio [19]:

$$K_{1-2} = \frac{k_{1-2}+1}{k_{1-2}-1} \quad (17)$$

Here, T_{1-2} and x_{1-2} are the average temperature and heat-release fraction over the interval considered; λ is the excess-air ratio. This approximately accounts for changes in the thermophysical properties of the working fluid as the initial mixture is converted into combustion products.

Thus, variable thermophysical properties averaged over elementary intervals are used in the calculation.

The current molar volume of the working fluid is:

$$V_\beta = M_a \cdot \left(1 + \frac{m_H \cdot x}{19{,}04 \cdot \lambda \cdot \left(n_C + \frac{m_H}{4} \right)} \right) \quad (18)$$

For dual-fuel operation, the current molar volume of the working fluid is determined taking the substitution coefficient k_r into account:

$$V_{\beta g} = M_a \cdot \left\{ 1 + \frac{\left(m_{Hd} + k_r \cdot (m_{Hg} - m_{Hd}) \right) \cdot x}{19{,}04 \cdot \lambda_{gd} \cdot \left[m_{Cd} + k_r \cdot (m_{Cg} - m_{Cd}) + \frac{m_{Hd} + k_r \cdot (m_{Hg} - m_{Hd})}{4} \right]} \right\} \quad (19)$$

Residual gases are taken into account when determining the total charge quantity at the end of intake:

$$M_a = M_1 \cdot (1+\gamma_r) \quad (20)$$

where γ_r is the residual-gas coefficient. In this way, the results of cylinder filling and scavenging are included in the initial conditions for calculating compression and combustion.

The effect of gas exchange is accounted for integrally when determining the quantity and state of the working fluid in the cylinder. The fresh-charge quantity is determined from the cylinder displacement, volumetric efficiency, charge density and molar mass:

$$M_1 = \frac{V_h \cdot \eta_v \cdot \rho_0}{\mu_{\text{mix}}} \quad (21)$$

During combustion, changes in the molar quantity and composition of the working fluid are additionally accounted for using the functions $f = V_{\beta d}(\varphi)$, $f = V_{\beta gd}(\varphi)$, $f = \mu_{mixd}(\varphi)$, and $f = \mu_{mixgd}(\varphi)$. These relationships contain the heat-release fraction x, excess-air ratio λ and fuel elemental-composition characteristics; the

substitution coefficient k_r is also included for dual-fuel operation. The resulting characteristics are used to calculate the state and specific volume of the working fluid.

The current molecular mass of gases in the diesel cycle is:

$$\mu_{mix} = \frac{44,01 \cdot n_C \cdot x + 9,01 \cdot x \cdot m_H + 32 \cdot \left(n_C + \frac{m_H}{4} \right) \cdot (\lambda - x) + 105,844 \cdot \lambda \cdot \left(n_C + \frac{m_H}{4} \right)}{4,76 \cdot \lambda \cdot \left(n_C + \frac{m_H}{4} \right) + \frac{m_H \cdot x}{4}} \tag{22}$$

The molecular mass of gases in the dual-fuel cycle is:

$$\mu_{mixg} = \frac{\left(n_{Cd} + k_r \cdot (n_{Cg} - n_{Cd}) \right) \cdot (12,01 \cdot x + 137,844 \cdot \lambda_{gd}) + \left(m_{Hd} + k_r \cdot (m_{Hg} - m_{Hd}) \right) \cdot (1,01 \cdot x + 34,461 \cdot \lambda_{gd})}{4,76 \cdot \lambda_{gd} \cdot \left(n_{Cd} + k_r \cdot (n_{Cg} - n_{Cd}) \right) + \frac{\left(m_{Hd} + k_r \cdot (m_{Hg} - m_{Hd}) \right) \cdot x}{4}} \tag{23}$$

Specific volume in the diesel cycle:

$$\begin{aligned} v_i = \{ & 2,8715 \cdot 10^{-4} \cdot \left[T_0 + \Delta T + \left(\varphi_c \cdot p_r \cdot (T_0 + \Delta T) \cdot \left\langle \varphi_{c.ad} \cdot \varepsilon \cdot p_0 \cdot \left(1 - \left(\beta_{in}^2 + \xi_{in} \right) \cdot n^2 \cdot \pi^2 \cdot S^2 \cdot D^2 \cdot \left(1 + \alpha^2 \right) \cdot 3,024557 \cdot \right. \right. \right. \right. \\ & \left. \left. \left. \left. \cdot 10^2 \cdot h_v^{-2} \cdot \left(d_n \cdot \cos \alpha_v + h_v \cdot \alpha_v \cdot \cos^2 \alpha_v \right)^{-2} \cdot T_0^{-1} \right) - \varphi_c \cdot p_r \right\rangle^{-1} \right] \cdot \left[1 + \varphi_c \cdot p_r \cdot (T_0 + \Delta T) \cdot \left\{ \varphi_{c.ad} \cdot \varepsilon \cdot \left[p_0 \cdot \right. \right. \right. \\ & \left. \left. \left. \cdot \left(1 - \left(\beta_{in}^2 + \xi_{in} \right) \cdot n^2 \cdot \pi^2 \cdot S^2 \cdot D^4 \cdot \left(1 + \alpha^2 \right) \cdot 3,024557 \cdot 10^2 \cdot h_v^{-2} \cdot \left(d_n \cdot \cos \alpha_v + h_v \cdot \alpha_v \cdot \cos^2 \alpha_v \right)^{-2} \cdot T_0^{-1} \right)^{-1} - \varphi_c \cdot p_r \right\}^{-1} \cdot \right. \right. \\ & \left. \left. \cdot T_r^{-1} \right]^{-1} \cdot p_0^{-1} \cdot \left(1 - \left(\beta_{in}^2 + \xi_{in} \right) \cdot n^2 \cdot \pi^2 \cdot S^2 \cdot D^4 \cdot \left(1 + \alpha^2 \right) \cdot 3,024557 \cdot 10^2 \cdot h_v^{-2} \cdot \left(d_n \cdot \cos \alpha_v + h_v \cdot \alpha_v \cdot \cos^2 \alpha_v \right)^{-2} \cdot T_0^{-1} \right)^{-1} \cdot \right. \\ & \left. \cdot \varepsilon^{-1} \cdot \left\{ 1 + (\varepsilon - 1) \cdot 2^{-1} \cdot \left[1 + \alpha^{-1} - \left(\cos \varphi + \alpha^{-1} \cdot \sqrt{1 - \alpha^2 \cdot \sin^2 \varphi} \right) \right] \right\} \end{aligned} \tag{24}$$

Specific volume in the dual-fuel cycle:

$$\begin{aligned} v_{ig} = \{ & 0,8316 \cdot 10^{-2} \cdot \left[T_0 + \Delta T + \left(\varphi_c \cdot p_r \cdot (T_0 + \Delta T) \cdot \left\langle \varphi_{c.ad} \cdot \varepsilon \cdot p_0 \cdot \left(1 - \left(\beta_{in}^2 + \xi_{in} \right) \cdot n^2 \cdot \pi^2 \cdot S^2 \cdot D^2 \cdot \left(1 + \alpha^2 \right) \cdot 3,024557 \cdot \right. \right. \right. \right. \\ & \left. \left. \left. \left. \cdot 10^2 \cdot h_v^{-2} \cdot \left(d_n \cdot \cos \alpha_v + h_v \cdot \alpha_v \cdot \cos^2 \alpha_v \right)^{-2} \cdot T_0^{-1} \right) - \varphi_c \cdot p_r \right\rangle^{-1} \right] \cdot \left[1 + \varphi_c \cdot p_r \cdot (T_0 + \Delta T) \cdot \left\{ \varphi_{c.ad} \cdot \varepsilon \cdot \left[p_0 \cdot \right. \right. \right. \\ & \left. \left. \left. \cdot \left(1 - \left(\beta_{in}^2 + \xi_{in} \right) \cdot n^2 \cdot \pi^2 \cdot S^2 \cdot D^4 \cdot \left(1 + \alpha^2 \right) \cdot 3,024557 \cdot 10^2 \cdot h_v^{-2} \cdot \left(d_n \cdot \cos \alpha_v + h_v \cdot \alpha_v \cdot \cos^2 \alpha_v \right)^{-2} \cdot T_0^{-1} \right)^{-1} - \varphi_c \cdot p_r \right\}^{-1} \cdot \right. \right. \\ & \left. \left. \cdot T_r^{-1} \right]^{-1} \cdot p_0^{-1} \cdot \left(1 - \left(\beta_{in}^2 + \xi_{in} \right) \cdot n^2 \cdot \pi^2 \cdot S^2 \cdot D^4 \cdot \left(1 + \alpha^2 \right) \cdot 3,024557 \cdot 10^2 \cdot h_v^{-2} \cdot \left(d_n \cdot \cos \alpha_v + h_v \cdot \alpha_v \cdot \cos^2 \alpha_v \right)^{-2} \cdot T_0^{-1} \right)^{-1} \cdot \right. \\ & \left. \cdot \left[\left(n_{Cd} + k_r \cdot \left(n_{Cg} - n_{Cd} \right) \right) \cdot 137,844 + \left(m_{Hd} + k_r \cdot \left(m_{Hg} - m_{Hd} \right) \right) \cdot 34,461 \right] \cdot \left[4,76 \cdot \left(n_{Cd} + k_r \cdot \left(n_{Cg} - n_{Cd} \right) \right) \right]^{-1} \cdot \right. \\ & \left. \cdot \varepsilon^{-1} \cdot \left\{ 1 + (\varepsilon - 1) \cdot 2^{-1} \cdot \left[1 + \alpha^{-1} - \left(\cos \varphi + \alpha^{-1} \cdot \sqrt{1 - \alpha^2 \cdot \sin^2 \varphi} \right) \right] \right\} \end{aligned} \tag{25}$$

Thus, the developed mathematical model provides an integrated description of combustion and the working process in diesel and dual-fuel operation. It accounts for the variable combustion-shape exponent, heat-release dynamics, fuel elemental composition, excess-air ratio, residual gases, gas exchange, working-medium properties, and the diesel-fuel substitution coefficient. The obtained relationships form the basis for calculating and comparing the heat-release fraction and rate, cylinder pressure and temperature, and for assessing changes in the engine working process during the transition to dual-fuel operation.

6. MATHEMATICAL MODELLING RESULTS

The calculated exponent m and heat-release fraction are shown in Figs. 1 and 2.

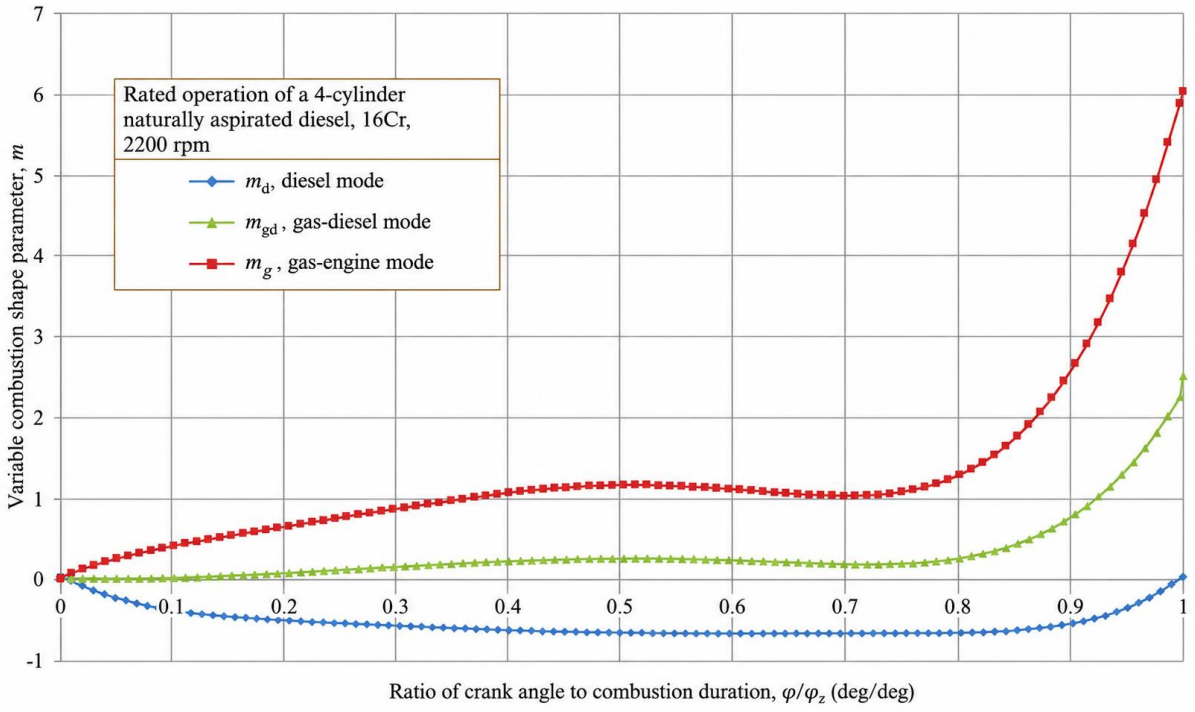


Fig. 1. Variation of the combustion exponent with crank angle.

The exponent m is predominantly negative for the diesel cycle and positive for the dual-fuel cycle (Fig. 1).

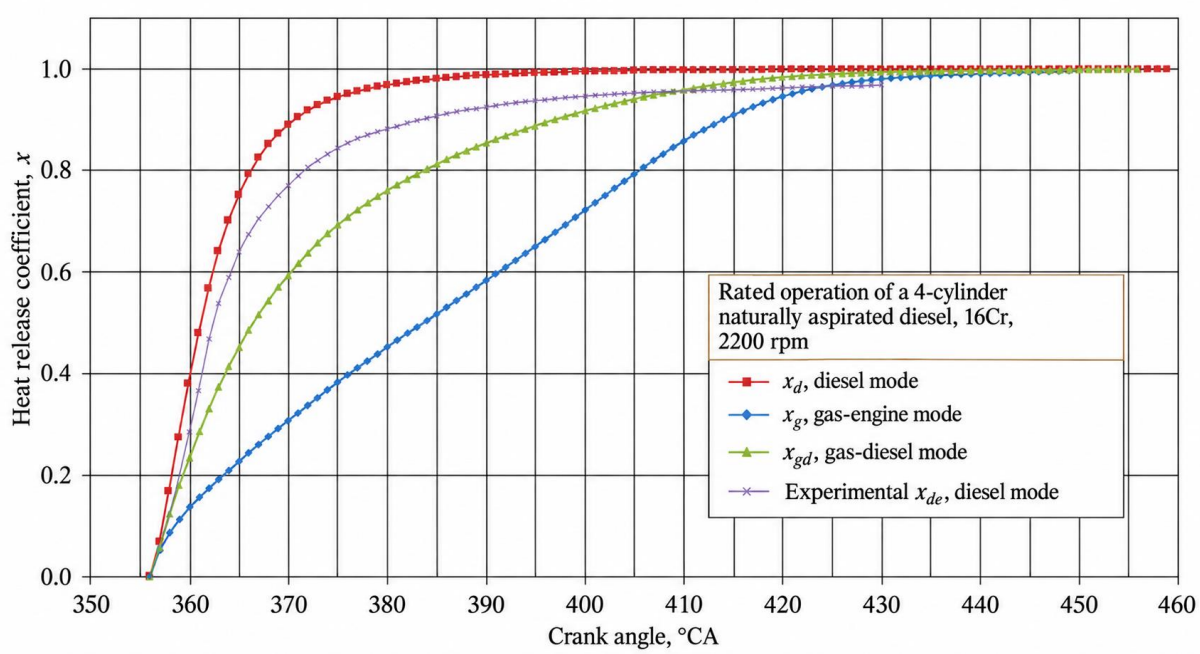


Fig. 2. Integral heat-release characteristics.

The heat-release rate $\frac{dx}{d\varphi}$ is obtained by differentiating the heat-release fraction with respect to crank angle, giving the differential characteristics shown in Fig. 3.

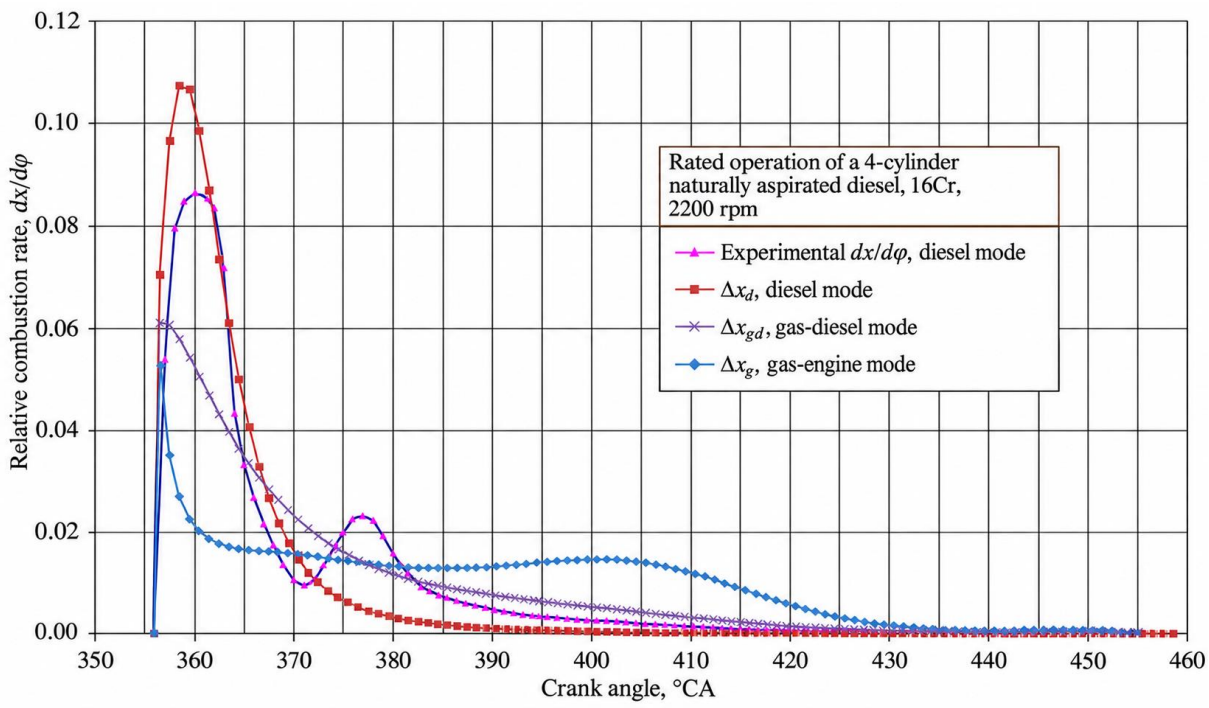


Fig. 3. Differential heat-release characteristics.

The indicated parameters of the diesel and dual-fuel cycles are shown in Fig. 4.

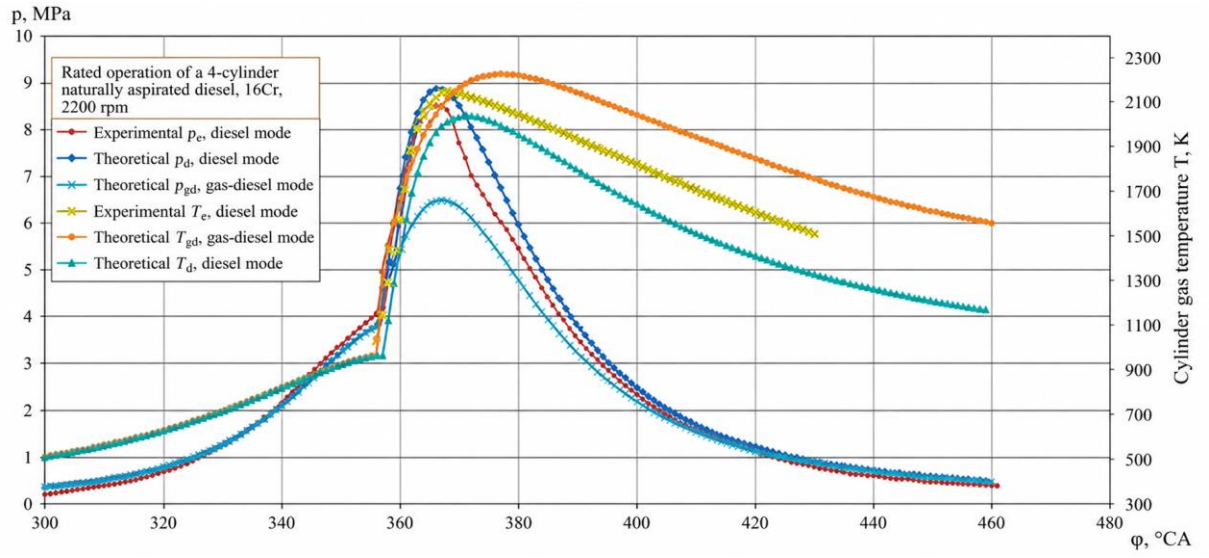


Fig. 4. Cylinder gas pressure and temperature versus crank angle for the diesel and dual-fuel cycles of the 4Ch11.0/12.5 engine.

The calculations predict a lower peak pressure and a higher maximum temperature for the dual-fuel cycle (Fig. 4). The results indicate the need to coordinate gas supply and pilot-fuel quantity [23]; a substitution coefficient $k_r = 0.5$ was used in the model.

The theoretical and experimental diesel-cycle characteristics (Figs. 2–4) were compared at the rated operating mode of 2200 rpm.

The normalised root mean square error (NRMSE) was used for quantitative comparison:

$$\delta_{\mathrm{RMS},j}=\frac{\sqrt{\frac{1}{n_j}\sum_{i=1}^{n_j}\left(y_{\mathrm{th},i,j}-y_{\mathrm{exp},i,j}\right)^2}}{y_{\max,j}-y_{\min,j}}\cdot 100\% \qquad (26)$$

where $y_{th,i,j}$ and $y_{\mathrm{exp},i,j}$ are, respectively, the theoretical and experimental values of the *j*-th characteristic at the i-th comparison point; n_j is the number of value pairs; and $y_{\max,j}$ and $y_{\min,j}$ are the deviation limits adopted in the calculation and presented in Table 4.

Table 4

Comparison errors for theoretical and experimental diesel-cycle characteristics

Characteristic	Fig.	$y_{\min}$	$y_{\max}$	RMSE	NRMSE, %
Heat-release fraction *x*	2	0	0.998784	0.070375	7.05
Heat-release rate $dx/d\varphi$ $(°CA)^{-1}$	3	0	0.107070	0.017066	15.94
Pressure *p* (MPa)	4	0.373001	8.880019	0.275024	3.23
Temperature *T* (K)	4	964.2673	2045.2418	159.9321	14.80

The maximum normalised root mean square error among the considered characteristics is 15.94%, corresponding to the heat-release rate (Fig. 3). The lowest value, 3.23%, was obtained for pressure. These estimates quantitatively characterise the differences between the experimental and theoretical diesel-cycle curves at the rated operating mode.

The substitution coefficient k_r accounts for the reduction in the cyclic share of heat released by diesel combustion and its replacement by the cyclic share from gaseous fuel in the dual-fuel cycle. In the theoretical study, $k_r = 0.5$, i.e. 50% substitution, was adopted on the basis of the literature review. Analysis of the theoretical indicator diagrams $p_d = f(\varphi)$ for the diesel cycle and $p_{gd} = f(\varphi)$ for the dual-fuel cycle showed a peak diesel-cycle pressure $p_{zd} = 8.88$ MPa at $\varphi_{zd} = 366^\circ$, compared with $p_{zgd} = 6.495$ MPa at $\varphi_{zgd} = 367^\circ$ for the dual-fuel cycle, and a maximum diesel-cycle temperature $T_{zd} = 2045$ K at $\varphi_{zd} = 371^\circ$, compared with $T_{zd} = 2227$ K at $\varphi_{zd} = 377^\circ$ for the dual-fuel cycle. Therefore, mathematical modelling of the diesel and dual-fuel engine working cycles indicates that, with other operating conditions equal, the dual-fuel-cycle diagram shows lower efficiency. Increasing the substitution coefficient k_r with other conditions equal is therefore inadvisable, whereas decreasing it moves away from the objective of determining the maximum diesel substitution coefficient. This creates a contradiction to resolve: increase k_r, at the expense of efficiency, or decrease k_r at the expense of substitution. In addition, the mathematical model investigated diesel and dual-fuel engine cycles under standard atmospheric conditions at the rated operating mode. Further investigation of k_r therefore requires experiments that account for the actual atmospheric parameters of the working fluid and different engine operating modes.

7. DISCUSSION OF RESULTS

The mathematical modelling results shown in Figs. 1–4 characterise the patterns of combustion and heat release, as well as changes in cylinder pressure and temperature in the diesel and dual-fuel cycles at the rated operating condition. Quantitative comparison of the calculated characteristics with the experimental diesel-cycle curves (Table 4) defines the model accuracy limits, while comparison of the two calculated cycles reflects changes in the working process during the transition to dual-fuel operation.

The transition to dual-fuel operation at a substitution coefficient $k_r = 0.5$ changes the variable combustion-shape exponent characteristic and redistributes heat release over the crankshaft angle (Figs. 1–3). Under the adopted identical initial conditions, the dual-fuel cycle is characterised by a lower calculated maximum pressure but a higher maximum temperature than the diesel cycle (Fig. 4). In study [8], an increase in maximum pressure and heat-

release intensity was recorded under different operating conditions. The difference is associated with load, excess-air ratio, pilot-fuel quantity, mixture-formation method and combustion duration, which determine the effect of LPG on the working process.

The NRMSE values are 7.05% for the integral heat-release fraction, 15.94% for the heat-release rate, 3.23% for pressure and 14.80% for temperature (Table 4). The best agreement was obtained for the pressure curve, whereas the greatest deviation was characteristic of the differential heat-release characteristic. The maximum value of 15.94% defines the existing accuracy limit of the model when applied at the rated operating condition and indicates satisfactory adequacy of the mathematical model.

In the mathematical model, mass exchange between thermodynamic systems is taken into account in integral form when determining the quantity and state of the working medium in the cylinder. The amount of fresh charge is determined through cylinder displacement, volumetric efficiency, charge density and molar mass, while the total charge quantity at the end of intake is determined with allowance for the residual-gas coefficient according to relationships (20) and (21). During combustion, changes in the molar quantity and composition of the working medium are taken into account by the relationships $f = V_{\beta d}(\varphi)$, $f = V_{\beta gd}(\varphi)$, $f = \mu_{mixd}(\varphi)$ and $f = \mu_{mixgd}(\varphi)$, which include the heat-release fraction x, excess-air ratio λ, elemental fuel composition and, for the dual-fuel cycle, substitution coefficient k_r. These characteristics are used to calculate the state and specific volume of the working medium.

This method of accounting for gas exchange provides a comparative calculation of the diesel and dual-fuel cycles of the investigated naturally aspirated diesel engine under the adopted operating conditions. Verification of the established patterns under load and speed conditions is the subject of the second part of the study.

In addition, according to equations (12) and (13), the calculated values of the total specific utilised heat of combustion for the diesel cycle, $q_z = 388.16$ kJ/kg, and for the dual-fuel cycle, $q_{zn} = 323.91$ kJ/kg, are determined with allowance for the excess-air ratios $\lambda_d = 1.51$ and $\lambda_{gd} = 1.54$, substitution coefficient $k_r = 0.5$ and working-medium composition. Therefore, gas supply and pilot-fuel quantity must be coordinated with the actual operating conditions; fuel efficiency should be evaluated from the consumption of both fuels, while energy efficiency should be assessed as the ratio of useful engine work to the total energy supplied with diesel fuel and LPG.

The combination of the variable-exponent I. I. Wiebe model with its quantitative comparison against the experimental diesel-cycle curves characterises the dual-fuel process of a production naturally aspirated diesel engine with external LPG mixture formation. The obtained relationships can be used for the initial selection of gas supply and pilot-fuel quantity and for the development of control devices and algorithms. Experimental refinement of these relationships for load and speed conditions is presented in the second part of the study.

8. CONCLUSIONS

The variable-exponent I. I. Wiebe model, supplemented by relationships for the excess-air ratio, residual gases, gas exchange, working-medium composition and variable heat capacity, was used to calculate heat release, pressure and temperature in the diesel and dual-fuel operating modes of the 4Ch11.0/12.5 naturally aspirated diesel engine.

At the theoretical substitution coefficient k_r = 0.5, redistribution of heat release, a lower calculated maximum pressure and a higher maximum temperature were established in the dual-fuel cycle compared with the diesel cycle under the adopted identical initial conditions. This confirms the need for coordinated regulation of LPG supply and pilot-fuel quantity.

Comparison with the experimental diesel-cycle curves at a rotational speed of 2200 rpm yielded NRMSE values of 3.23% for pressure, 7.05% for the heat-release fraction, 14.80% for temperature and 15.94% for the heat-release rate. Thus, the maximum relative root-mean-square error was 15.94%, which indicates the adequacy of the mathematical model.

For equal fuel mass fractions, the calculated LPG energy fraction is approximately 51.9%, owing to the different lower heating values of diesel fuel and LPG. Therefore, assessment of fuel and energy efficiency requires the consumption and lower heating values of both fuels to be taken into account.

The obtained relationships provide a basis for refining the dual-fuel working-process model and developing algorithms for controlling gas supply and pilot-fuel quantity. Experimental verification

of the modelling results under load and speed conditions is the subject of the second part of the study.

References

[1] Kovalev, S. O. (2019). Development and research of the D-240-LPG gas engine converted from a tractor diesel engine. Internal Combustion Engines, (2), 18-25.

[2] Aydin, M., Irgin, A., & Çelik, M. B. (2018). The impact of diesel/LPG dual fuel on performance and emissions in a single cylinder diesel generator. Applied Sciences, 8(5), 825.

[3] Mohsen J. M., Al-Dawody M. F. (2022). The combustion characteristics of compression ignition engine fuelled partially by LPG-Diesel blends (Simulation study). Al-Qadisiyah Journal for Engineering Sciences, 15(3), 156-163.

[4] Liu, J., & Dumitrescu, C. E. (2018). Flame development analysis in a diesel optical engine converted to spark ignition natural gas operation. Applied Energy, 230, 1205-1217.

[5] Bari, S., & Hossain, S. N. (2019). Performance of a diesel engine run on diesel and natural gas in dual-fuel mode of operation. Energy Procedia, 160, 215-222.

[6] Tang, D., Liu, N., Wang, J., Zhao, C., & Luo, F. (2020). Effect of load on combustion cyclic variation in CNG/diesel dual-fuel engine. International Journal of Energy for a Clean Environment, 21(1), 25–39.

[7] Toledo, E., Guerrero, F., Amador, G., & Toledo, M. (2022). Experimental assessment of the performance and fine particulate matter emissions of a LPG-diesel dual-fuel compression ignition engine. Energies, 15(23), 9035. https://doi.org/10.3390/en15239035

[8] Tchato Yotchou, G. V., Issondj Banta, N. J., Kabini Karanja, S., & Ngayihi Abbe, C. V. (2023). Experimental study on the effect of load and air+gas/fuel ratio on the performances, emissions and combustion characteristics of diesel–LPG fuelled single stationary CI engine. Engineering Reports, 5(9), e12654. https://doi.org/10.1002/eng2.12654

[9] Maza Rubina, A., & Lastra Espinoza, L. (2006). Developing of the thermal calculation of the gasodiesel engine with internal formation of the mix air gas and validation by the experimentation. Tecnia. 16(2), 93–108.

[10] Li, T., Zhao, P., He, H., Wang, C., Zhang, H., Chen, Z., & Chen, H. (2025). Dual-fuel dual-direct injection: An efficient and clean combustion technology for diesel engines. Journal of the Energy Institute, 119, 102006. https://doi.org/10.1016/j.joei.2025.102006

[11] Belousov, E., Marchenko, A., Gritsuk, I. V., Savchuk, V., Bulgakov, N., Mitienkova, V., Ahieiev, M., Samarin, O., Vrublevskyi, R., Volodarets, M., Kalashnikov, Y., & Pronin, S. (2020). Research of the gas fuel supply process on the compression stroke in ship's low-speed gas-diesel engines. SAE Technical Paper 2020-01-2107. https://doi.org/10.4271/2020-01-2107

[12] Zhang, C., Zhao, W., Miao, T., & Wu, H. (2016). Development and application of a control scheme to reduce insufficient operation of an NG-diesel dual-fuel automobile. Proceedings of the Institution of Mechanical Engineers, Part D: Journal of Automobile Engineering, 230(1), 61–69. https://doi.org/10.1177/0954407015578039

[13]Marchenko, A. P., Parsadanov, I. V., & Dmytrychenko, M. F. (2014). Dvyhuniv vnutrishnyoho zhorannya: Vol. 1. Teoriya robochykh protsesiv [Internal combustion engines: Vol. 1. Theory of working processes] (A. P. Marchenko, Ed.). NTU "KhPI".

[14]Babych, O. S. (2003). Prystriy dlya rehulyuvannya potuzhnosti hazodyzelya (UA 52926 C2).

[15] Kovalev, S., & Patlatyuk, K. Development and Research of a Gasodiesel Control System with a Diesel Fuel "Ignition Dose" Corrector. Scientific Collection "InterConf+" , (37), 331-341.

[16] Jeong, D. S., Suh, S. W., Oh, S. M., & Choi, K. N. (1993, November). Development of a Mechanical CNG-Diesel Dual Fuel Supply System. In Seventh International Pacific Conference and Exposition on Automotive Engineering.

[17] Ergenç, A. T., & Koca, D. Ö. (2014). PLC controlled single cylinder diesel-LPG engine. Fuel, 130, 273-278.

[18] Willi, M. L. (1998). U.S. Patent No. 5,771,857. Washington, DC: U.S. Patent and Trademark Office.

[19] Vibe, I. I. (1962). Novoye o rabochem tsikle dvigateley. Mashgiz.

[20] Linkov, O. Yu. (2004). Selection and justification of mixture formation and combustion parameters in a high-speed diesel engine operating on alternative fuel (Extended abstract of Candidate's thesis, National Technical University "Kharkiv Polytechnic Institute").

[21] Razleytsev, N. F. (1980). Modelirovanie i optimizatsiya rotsessa sgoraniya v dizelyakh. Vyshcha Shkola.

[22] Marchenko, A. P., Osetrov, A. A., & Lynkov, O. Yu. (2013). Mathematical model of the fuel combustion process in a diesel engine. Internal combustion engines , (1).

[23] Hall, C., & Kassa, M. (2021). Advances in combustion control for natural gas–diesel dual fuel compression ignition engines in automotive applications: A review. Renewable and Sustainable Energy Reviews, 148, 111291.

[24] Fawole O. G., Cai X. M., Mackenzie A. R. Gas flaring and resultant air pollution: A review focusing on black carbon. Environmental Pollution. 2016. Vol. 216. P. 182–197. DOI: 10.1016/j.envpol.2016.05.075.

[25]Kuzmenko, A. P. (2012). Improving the performance of a small-displacement gas engine with spark ignition by selecting parameters that determine the combustion process (Doctoral dissertation, degree of Candidate of Technical Sciences: speciality 05.05. 03 "Engines and power plants" / A. P. Kuzmenko).

Information about authors.



Lysenko Roman, PhD Student in Industrial Mechanical Engineering, Department of Agroengineering and Technical Service. Research interests: diesel engines, petrol engines, alternative sources.
ORCID: https://orcid.org/0009-0007-9867-5581
E-mail: romandmytrovich@gmail.com



Ryaboshapka Vadym, Candidate of Technical Sciences, Associate Professor, Department of Agroengineering and Technical Service. Research interests: biofuels, internal combustion engines, tractors and automobiles.
https://orcid.org/0000-0003-1812-1030
E-mail: vadymryaboshapka@gmail.com